

A NEW METHOD OF X-RAY CRYSTAL ANALYSIS.¹

BY A. W. HULL.

THE beautiful methods of crystal analysis that have been developed by Laue and the Braggs are applicable only to individual crystals of appreciable size, reasonably free from twinning and distortion, and sufficiently developed to allow the determination of the direction of their axes. For the majority of substances, especially the elementary ones, such crystals cannot be found in nature or in ordinary technical products, and their growth is difficult and time-consuming.

The method described below is a modification of the Bragg method, and is applicable to all crystalline substances. The quantity of material required is preferably .005 c.c., but one tenth of this amount is sufficient. Extreme purity of material is not required, and a large admixture of (uncombined) foreign material, twenty or even fifty per cent., is allowable provided it is amorphous or of known crystalline structure.

OUTLINE OF METHOD.

The method consists in sending a narrow beam of monochromatic X-rays (Fig. 2) through a disordered mass of small crystals of the substance to be investigated, and photographing the diffraction pattern produced. Disorder, as regards orientation of the small crystals, is essential. It is attained by reducing the substance to as finely divided form as practicable, placing it in a thin-walled tube of glass or other amorphous material, and keeping it in continuous rotation during the exposure.² If the particles are too large, or are needle-shaped

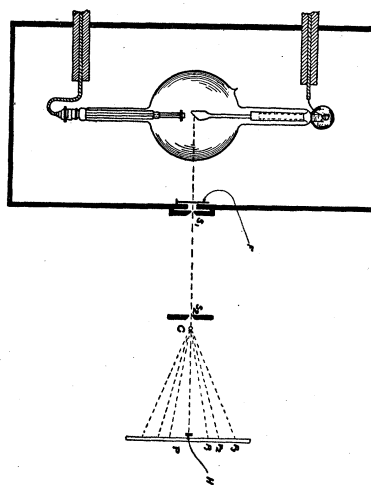


Fig. 2.

¹ A brief description of this method was given before the American Physical Society in October, 1916, and published in this journal for January, 1917.

² If the powder is fine, rotation is not necessary unless great precision is desired. With crystal grains .01 cm. in diameter, or less, the pattern generally appears quite uniform without rotation.

or lamellar, so that they tend to assume a definite orientation, they are frequently stirred. In this way it is assured that the average orientation of the little crystals during the long exposure is a random one. At any given instant there will be a certain number of crystals whose 100 planes make the proper angle with the X-ray beam to reflect the particular wave-length used, a certain number of others whose 111 planes are at the angle appropriate for reflection by these planes, and so for every possible plane that belongs to the crystal system represented. Each of these little groups will contain the same number of little crystals, provided the distribution is truly random, and the total number of crystals sufficiently large. This condition is very nearly realized in the case of fine powders, and may, by sufficient rotation and stirring, always be realized for the *average orientation* during the whole exposure; that is, there will be, *on the average*, as many cubic centimeters of crystals reflecting from their 100 planes as there are cubic centimeters reflecting from 111, 210, or any other plane. This is true for every possible plane in the crystal.

The diffraction pattern should contain, therefore, reflections from every possible plane in the crystal, or as many of these as fall within the limits of the photographic plate. Fig. 1, Plate I, shows the pattern given by aluminium when illuminated by a small circular beam of nearly monochromatic rays from a molybdenum tube. The exposure was nine hours, with 37 milliamperes at 30,000 volts, and crystal powder 15 cm. from the target and 5.9 cm. from photographic plate. The faintness of the vertical portions of the circles is due to the cylindrical form in which the powder was mounted, causing greater absorption of rays scattered in the vertical plane. Patterns containing many more lines are shown in Figs. 6-10, where the diaphragm limiting the beam was a slit instead of a circular aperture, and the pattern was received on a photographic film bent in the arc of a circle.

The number of possible planes in any crystal system is infinite. Hence if equal reflecting opportunity meant equal reflected energy, it would follow that the energy reflected by each system of planes must be an infinitesimal fraction of the primary beam, and hence could produce no individual photographic effect. It is easily seen, however, that only those planes whose distance apart is greater than $\lambda/2$, where λ is the wave-length of the incident rays, can reflect any energy at all. Planes whose distance apart is less than this cannot have, in any direction, except that of the incident beam, equality of phase of the wavelets diffracted by electrons in consecutive planes. Hence the resultant amplitude associated with any such plane is very small, and would be identically zero for a perfect

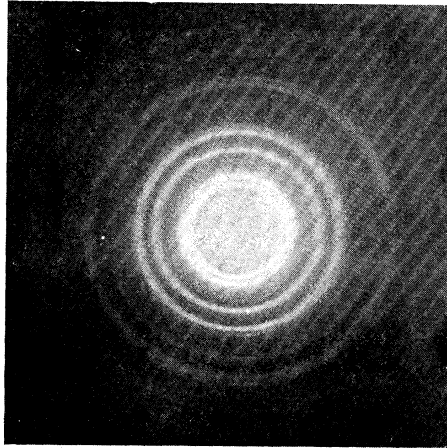


FIG. 1. Aluminium.

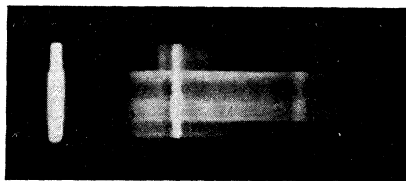


FIG. 5. Tungsten X-Ray Spectrum.

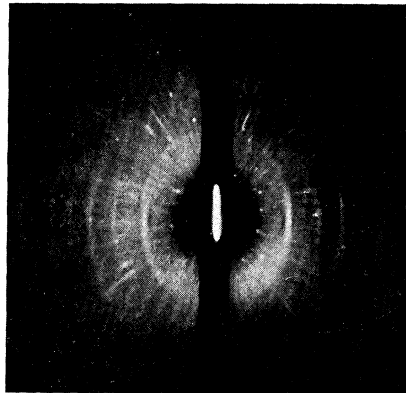


FIG. 6. Iron.



FIG. 7a. Silicon Steel.

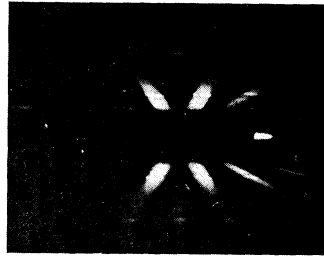


FIG. 7b. Silicon Steel.

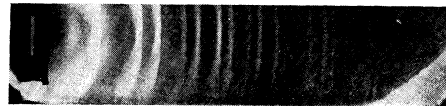


FIG. 8. Silicon.



FIG. 9. Aluminum.



FIG. 10. Magnesium.



FIG. 11. Graphite.



FIG. 12. Diamond.

A. W. HULL.

lattice and sufficiently large number of planes. The total scattered energy is therefore divided among a finite number of planes, each of which produces upon the photographic plate a linear image of the source (cf. Fig. 1). The total possible number of these lines depends upon the crystal structure and the wave-length. For diamond, with the wave-length of the K_{α} doublet of molybdenum, $\lambda = 0.712$, the total number of lines is 27. All of these are present in the photograph shown in Fig. 12. For the rhodium doublet, $\lambda = 0.617$, the total number is 30; for the tungsten doublet, $\lambda = 0.212$, it is more than 100; while the iron doublet, $\lambda = 1.93$, can be reflected by only three sets of diamond planes, the octahedral (111), rhombic dodecahedral (110), and the trapezohedral (311). The diffraction pattern in this case would consist, therefore, of but three lines.

The positions of these lines, in terms of their angular deviation from the central beam, are completely determined by the spacing of the corresponding planes, according to the classic equation $n\lambda = 2d \sin \theta$, where θ is the angle between the incident ray and the plane, hence 2θ is the angular deviation, d the distance between consecutive planes, λ the wave-length of the incident rays, and n the order of the reflection. The calculation of these positions is discussed in detail below.

The relative intensity of the lines, when corrected for temperature, angle, and the number of coöperating planes, depends only upon the space distribution of the electrons of which the atoms are composed. Most of these electrons are so strongly bound to their atoms that their positions can probably be completely specified by the positions of the atomic nuclei and the characteristic *structure* of the atom. Experiments are in progress to determine such a structure for some of the simpler atoms. A few of the electrons, however, are so influenced by the proximity of other atoms, that their position will depend much on the crystal structure and state of combination of the substance. There is also good reason to believe that certain electrons are really *free*, in that they belong to no atom, but occupy definite spaces in the lattice, as though they were atoms.

With elements of high atomic weight, where each atom contains a large number of electrons, the majority of these electrons must be quite close to the nucleus, so that the intensity of the lines will depend primarily upon the position of the nuclei relative to their planes, and only slightly upon the characteristic structure of the atom and the position of valence and free electrons. With these substances, therefore, the relative intensity of the lines gives direct evidence regarding the positions of the atoms, and may be used, in the manner described by the Braggs,¹ for the deter-

¹ X-Rays and Crystal Structure, pp. 120 ff.

mination of crystal structure. The powder photographs have an advantage, in this respect, over ionization-chamber measurements, in that the intensities of reflection from different planes, as well as different orders, are directly comparable, which is not true of ionization-chamber measurements unless the crystal is very large and may be ground for each plane.

In the case of light substances, on the other hand, the intensities depend very much on the internal structure of the atoms, and unless this structure is known or postulated, but little weight should be given to intensity in determining the crystal structure. Much evidence for the structure of these elements may be obtained, however, from the observation of the *position* of a large number of lines, and this evidence will generally be found sufficient. The examples given at the end of this paper are all elements of low atomic weight, and the analysis given is based entirely on the position of the lines. The photographs used for the analysis are preliminary ones, taken with very crude experimental arrangements, and yet in every case except one the evidence is sufficient.

The method of measuring and interpreting intensity will form the subject of a future paper.

EXPERIMENTAL ARRANGEMENT.

The arrangement of apparatus is shown in Fig. 2. The X-ray tube is completely enclosed in a very tightly built lead box. If a tungsten target is to be used this box should be of $\frac{1}{4}$ inch lead, with an extra $\frac{1}{4}$ inch on the side facing the photographic plate. If a rhodium or molybdenum target is used $\frac{1}{8}$ inch on the side toward the photographic plate, and $\frac{1}{16}$ inch for the rest of the box, is sufficient. The rays pass through the filter F and slits S_1 and S_2 , and fall upon the crystal substance C , by which they are diffracted to points p_1 , p_2 , etc., on the photographic plate P . The direct beam is stopped by a narrow lead strip H , of such thickness that the photographic image produced by this beam is within the range of normal exposure. For a tungsten target, the thickness of this strip should be $\frac{1}{8}$ inch; for a molybdenum target about $\frac{1}{100}$ inch.

THE X-RAY TUBE.

In order to produce monochromatic rays, it is necessary to use a target which gives a characteristic radiation of the desired wave-length, and to run the tube at such a voltage that the radiation of this wave-length will be both intense and capable of isolation by filtering.

The relation between general and characteristic radiation at different voltages has been investigated, for tungsten and molybdenum, by the

author,¹ and, in more detail, for rhodium by Webster and platinum by Webster and Clark.² The results may be summarized as follows: The characteristic *line spectra* are excited only when the voltage across the tube is equal to or greater than the value $V = h\nu/e$, where h is Planck's constant, e the charge of an electron, and ν the frequency corresponding to the short wave-length limit of the series to which the line belongs.

With increase of voltage above this limiting voltage, the intensity of the lines increases rapidly, approximately proportional to the $3/2$ power of the excess of voltage above the limiting value.³ The following table will show the rate of increase for the α line of the K series of molybdenum, as used in the experiments described below.⁴

TABLE I.
Increase of Intensity of the K_{α} Line of Mo with Voltage.

	Kilovolts									
	20.	22.	24.	26.	28.	30.	32.	34.	36.	40.
Intensity.....	0	1.25	2.75	4.80	7.30	9.60	12.65	15.2	18.5	23.4

The rapid increase of characteristic radiation with voltage makes it desirable to use as high voltage as possible. If the voltage is too high, however, a part of the general radiation, whose maximum frequency is directly proportional to the voltage,⁵ becomes so short that it is impossible to separate it from the characteristic by a selective filter. With a molybdenum target the best working voltage is about 30,000 volts, with tungsten about 100,000 volts.

FILTERS.

Although it is impossible to produce truly monochromatic radiation by filtering, it is easy to obtain a spectrum containing only *one line*, and in which the intensity of this line is more than thirty times that of any part of the general radiation. To accomplish this, use is made of the sudden increase in absorption of the filter at the wave-length corresponding to the limit of one of its characteristic series; that is, at the wave-length which is just short enough to excite in the filter one of its characteristic radiations. A filter is chosen whose K series limit⁶ lies

¹ Nat. Acad. Proc., 2, 268, 1916.

² Phys. Rev., 7, 599, 1916; Nat. Acad. Proc., 3, 185, 1917.

³ Webster and Clark, Proc. Nat. Acad., 3, 185, 1917.

⁴ The general radiation of the same wave-length as the α line is included in these values.

⁵ See Duane and Hunt, Phys. Rev., 6, 619, and Hull, Phys. Rev., 7, 156.

⁶ A complete table of wave-lengths of series lines for all elements thus far investigated is given by Siegbahn, Ber. d. D. Phys. Gesel., 13, 300, 1917.

as close as possible to the desired wave-length *on its short wave-length side*. For example, to isolate the K lines of molybdenum whose wave-length is $.712 \text{ \AA}$., the most appropriate filter is zirconium, the limit of whose K series is at $\lambda = .690 \text{ \AA}$. The absorption coefficient of the filter is then a minimum for the wave-length in question, and increases rapidly with wave-length *in both directions*; on the left, toward shorter wave-lengths, it jumps suddenly by about 8-fold; on the right it increases more slowly, viz., as the cube of the wave-length.¹

If the longest wave-length in the series, which, fortunately, in the case of the K series, is the most intense, is chosen for the monochromatic ray, the eight-fold increase in absorption coefficient will completely eliminate the other lines of the series, while reducing the chosen line by only one-half. To eliminate the general radiation is not so easy. Webster has shown² that the intensity of the characteristic radiation increases more rapidly with voltage than that of the neighboring general radiation, so that the higher the voltage the more prominently the line

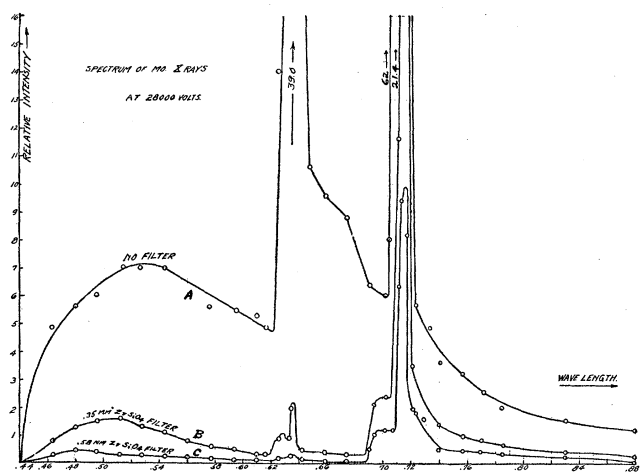


Fig. 3.

stands out above adjacent wave-lengths, and this is the only way in which it can be sharply separated *from longer wave-lengths*. If the voltage is too high, however, the shortest wave-length end of the general spectrum becomes transmissible by the filter, and while its wave-length is far removed from that of the line which is to be isolated, and it can itself produce no line image, yet its integral effect produces a general blackening of the plate that obscures the lines. Sharp limitation

¹ Hull and Rice, *PHYS. REV.*, 8, 326, 1916.

² L. c.

on the *short* wave-length side is obtained by the selective action of the filter.

It is necessary, therefore, to choose filter material, filter thickness, and voltage, to correspond to the target used. For a molybdenum target, the filter should be zirconium, and a thickness of about 0.35 mm. of powdered zircon is sufficient¹ (see Fig. 3). The optimum voltage is between 28,000 and 30,000 volts. For a tungsten target the filter should be ytterbium, of a thickness of about 0.15 mm., but this has not yet been tested. A filter of this thickness of metallic tungsten or tantalum eliminates most of the general spectrum, but leaves the β

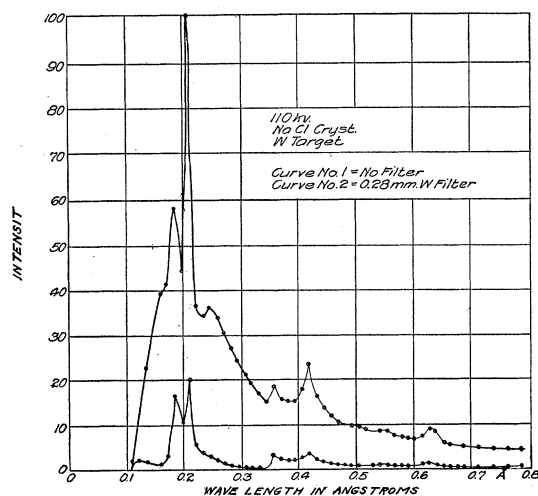


Fig. 4.

doublet as well as the α doublet, which is very undesirable (cf. Figs. 4 and 5). The optimum voltage is about 100,000 volts.

The effect of filtering on the spectrum of a molybdenum target at 28,000 volts is shown in Fig. 3, which gives the intensity of the different wave-lengths as measured with an ionization chamber, so constructed as to eliminate, nearly, errors due to incomplete absorption.² No correc-

¹ The absorption of the Si and O in zircon is negligible compared to that of the zirconium, so that crystal zircon is as efficient as metallic zirconium.

² The ionization chamber contains two electrodes of equal length. The second electrode, the one farther from the crystal, was connected to the electrometer, and the pressure of methyl iodide in the chamber was such that the wave-lengths in the middle of the range investigated suffered 50 per cent. absorption in passing through the first half of the chamber. The electrometer deflection is proportional to $I_0 e^{-\mu l} (1 - e^{-\mu l})$, where I_0 is the intensity on entering the chamber, l the length of either electrode and μ the coefficient of absorption of the methyl iodide. This expression has a very flat maximum for $e^{-\mu l} = \frac{1}{2}$, so that for a considerable range on either side, the readings are proportional to I_0 .

tion has been made for coefficient of reflection of the (rock salt) crystal. The intensities of the K lines are too great to be shown on the figure, the α line being four times and the β line two and one half times the height of the diagram. A filter of .35 mm. of zircon reduces the intensity of the α line from 62 to 21.4; while reducing the β line from 39 to 2.2. The general radiation to the left is still quite prominent. An increase in filter thickness from .35 mm. to .58 mm. (Curve *C*) reduces it but little more than it reduces the α line, so that very little is gained by additional filtering. The sudden increase in absorption of the zirconium is seen at $\lambda_0 = 0.690 \text{ \AA.}$, which is exactly the short wave-length limit of its K series, as extrapolated from Malmer's values of the β_1 and β_2 lines of yttrium and the β_1 line of zirconium.

The effect of a tungsten filter upon the spectrum of tungsten at 110,000 volts is shown in Figs. 4 and 5. Here the critical wave-length of the filter is at the short wave-length edge of the whole series, so that all the lines are present. A filter of ytterbium would eliminate all but the α doublet. Fig. 4 gives the ionization chamber measurements, uncorrected, of the tungsten spectrum at 110,000 volts, as reflected by a rock salt crystal. The upper curve is the unfiltered spectrum, the lower that which has passed through a filter of 0.15 mm. of metallic tungsten. The K lines are much more prominent in the filtered than in the unfiltered spectrum, but the general radiation, especially the short wave-length end, is much too prominent, showing that the voltage is too high. In Fig. 5 the effect of the tungsten filter (above) is compared with that of 1 cm. of aluminium (below), in order to show more clearly the selective effect of the tungsten filter. The wide middle portion of the spectrum is unfiltered.

THE CRYSTALLINE MATERIAL.

The Bragg method of X-ray crystal analysis is by far the simplest whenever single crystals of sufficient perfection are available. If, however, perfect order of crystalline arrangement cannot be had, the next simplest condition is perfect chaos, that is, a random grouping of small crystals, such that there is equi-partition of reflecting opportunity among all the crystal planes. This has two disadvantages, viz., that the opportunity of any one plane to reflect is very small, so that long exposures are necessary; and the images from all planes appear on the same plate, so that it is impossible, without calculation, to tell which image belongs to which plane. It has the advantages, on the other hand, of allowing a definite numerical calculation of the position and intensity of each line, and of being free from uncertainties due to imperfection and twinning of crystals. In the latter respect it serves as a valuable check on the direct Bragg method.

The crystalline material is, wherever possible, procured in the form of a fine powder of .01 cm. diameter or less. This may be accomplished by filing, crushing, or by chemical or electro-chemical precipitation, or by distillation. In the case of the metals like alkalis, to which none of these methods can be applied, satisfactory results have been obtained by squirting the metal through a die in the form of a very fine wire, which is packed, with random folding, into a small glass tube, and kept in continuous rotation, with frequent vertical displacements, during exposure.

The method of mounting the crystalline substance depends on the wave-length used. If tungsten rays ($\lambda = 0.212$) are used, so that the angles of reflection, for all visible lines, are small, it is most convenient to press the powder into a flat sheet, or between plane glass plates, and place this sheet at right angles to the beam. In this case the correction for the difference in absorption of the different diffracted rays is negligible. If a molybdenum tube is used, on the other hand, diffracted rays can be observed at angles up to 180° (cf. Fig. 10), so that the substance must be mounted in a cylindrical tube. In this case also, the correction for absorption is unnecessary, provided the diameter of the tube is properly chosen and the beam of rays is wide enough to illuminate the whole tube.

The optimum thickness of crystalline material, for a given wave-length, may be calculated approximately as follows:

Let k represent the scattering coefficient and μ the absorption coefficient of the substance for the wave-length used, and I_0 the intensity of the incident rays. The intensity scattered by a thin layer dx at a distance x below the surface will be

$$dR = kI_0e^{-\mu x}dx.$$

This radiation will suffer further absorption in passing through a thickness $t-x$, approximately, where t is the thickness of the sheet. Hence the total intensity of the scattered radiation that emerges will be

$$\begin{aligned} R &= \int_0^t kI_0e^{-\mu t}dx \\ &= kI_0te^{-\mu t}. \end{aligned}$$

This will be a maximum when

$$\frac{dR}{dt} = kI_0(e^{-\mu t} - \mu te^{-\mu t}) = 0$$

or

$$t = \frac{1}{\mu},$$

where t is the thickness of the crystalline sheet in centimeters and μ the linear absorption coefficient.

If the material is in cylindrical form, the optimum diameter is slightly greater than the above value.

EXPOSURE.

Very long exposures, as remarked above, are necessary if a large number of lines is desired, and it is important to increase the speed by the use of an intensifying screen, and by bringing the crystal as close as practicable to the tube. With rays as absorbable as those from a molybdenum tube, it is necessary to use films, not plates, with the intensifying screen. Under reasonable conditions, an exposure of ten to twenty hours will produce a general blackening of the plate well within the limit of normal exposure. Since a greater density than this cannot increase the contrast, nothing is to be gained by longer exposure. Further detail can be hoped for only by using more nearly monochromatic rays, screening the plate more perfectly from stray and secondary rays in the room, and decreasing the ratio of amorphous to crystalline material in the specimen under examination.

ANALYSIS OF THE PHOTOGRAPHS.

A. Cubic Crystals.

The method of deducing the crystal structure from the experimental data is very similar to that used by the Braggs, with this difference: In the Bragg method reflections from three or four known planes are observed, and a structure is sought which gives the spacings and intensities observed for these planes. In the method described above a single photograph is taken, containing reflections from a large number of unknown planes, and a structure is sought whose *whole pattern* of planes, arranged in the order of decreasing spacing and omitting none, fits the observed pattern. In both cases the method is one of trial and error, namely, to try one arrangement after another, beginning with the simplest, until one is found which fits.

CALCULATION OF THEORETICAL CRYSTAL SPACINGS.

The process of calculating the spacings of the planes in any assumed crystal structure is as follows: The positions of the atoms are specified by their coördinates with respect to the crystallographic axes. For example, a centered cubic lattice is represented by a system of atoms whose coördinate (x, y, z) are $\left\{ \begin{array}{l} m, n, p, \\ m + \frac{1}{2}, n + \frac{1}{2}, p + \frac{1}{2} \end{array} \right.$ where $m, n,$ and p assume all possible integral values, and the unit is the side of the elementary cube. The distance from any atom $x_1, y_1, z_1,$ to a plane whose (Miller) indices are h, k, l is, for rectangular axes,

$$d = \frac{hx_1 + ky_1 + lz_1 - 1}{\sqrt{h^2 + k^2 + l^2}}. \quad (1)$$

Since the family of planes parallel to h, k, l , contains all the atoms in the crystal, one of these planes must pass through the atom x_1, y_1, z_1 , so that d is the distance from the plane h, k, l to a plane parallel to it through x_1, y_1, z_1 . The "spacing" of the planes h, k, l , which is the smallest value of d that repeats itself, is found by substituting different values of the coördinates m, n, p for x_1, y_1, z_1 in equation (1), and observing the smallest value and periodicity of d . For example, to find the spacing of the 111 planes of the centered cubic lattice, place h, k, l each equal to 1, assume for m, n and p the values 0, 1, 2, 3, etc., and substitute in equation (1). All the atoms in the group m, n, p are found to lie in planes at distances $\frac{1}{\sqrt{3}}, \frac{2}{\sqrt{3}}, \frac{3}{\sqrt{3}}$, etc., from h, k, l , and those of the group $m + \frac{1}{2}, n + \frac{1}{2}, p + \frac{1}{2}$, at distances $\frac{1/2}{\sqrt{3}}, \frac{1\frac{1}{2}}{\sqrt{3}}, \frac{2\frac{1}{2}}{\sqrt{3}}$, etc. Since both groups contain the same number of atoms, the spacing is regular and is equal to $\frac{1/2}{\sqrt{3}}$ times the side of the elementary cube. If the structure is one of the fourteen regular lattices, as the centered cube, all parallel planes are equally spaced, and only the minimum value of d need be found.

In this way the spacings of all the principal planes, that is, those whose indices are small numbers, are calculated and tabulated; and it is easy, by systematic procedure, to be sure that no plane has been skipped whose spacing is within the limits of the table.

As an example, the calculation of the spacings of a face-centered lattice is given in full below (Table II.).

The coördinates of the atoms are

$$\begin{array}{l} m, \quad n, \quad p, \\ m + \frac{1}{2}, n + \frac{1}{2}, p, \\ m + \frac{1}{2}, n, \quad p + \frac{1}{2}, \\ m, \quad n + \frac{1}{2}, p + \frac{1}{2}, \end{array}$$

where m, n , and p assume all possible integral values.

The first column gives the indices of the form, the second the smallest value of d for that form, obtained by substituting the coördinates of the atoms in equation (1), and the third the same value of d expressed as a fraction of the lattice-constant, together with its submultiples $d/2, d/3, d/4$, etc., corresponding to reflections of second, third, etc., order. The unit is the "lattice constant," the side of the elementary face-centered

TABLE II.

Indices of Form.	Smallest Distance between Planes d .	Spacing of Planes and Submultiples d/n .		
		$n=1$.	2.	3.
100	$\frac{1}{\sqrt{1}}$.50	.25	.167
110	$\frac{1}{\sqrt{2}}$.354	.177	.118
111	$\frac{1}{\sqrt{3}}$.577	.289	.192
210	$\frac{1}{\sqrt{5}}$.224	.112	.075
310	$\frac{1}{\sqrt{10}}$.158	.079	.053
410	$\frac{1}{\sqrt{17}}$.121	.061	.040
320	$\frac{1}{\sqrt{13}}$.139	.070	.046
311	$\frac{1}{\sqrt{11}}$.302	.151	.101
411	$\frac{1}{\sqrt{18}}$.118	.059	.039
511	$\frac{1}{\sqrt{27}}$.192	.096	.064
711	$\frac{1}{\sqrt{51}}$.140	.070	.047
911	$\frac{1}{\sqrt{83}}$.110	.055	.037
322	$\frac{1}{\sqrt{17}}$.121	.061	.040
533	$\frac{1}{\sqrt{43}}$.152	.076	.051
733	$\frac{1}{\sqrt{67}}$.122	.061	.041
221	$\frac{1}{\sqrt{9}}$.167	.084	.056
331	$\frac{1}{\sqrt{19}}$.115	.058	.038
551	$\frac{1}{\sqrt{51}}$.140	.070	.047
553	$\frac{1}{\sqrt{59}}$.130	.065	.043
321	$\frac{1}{\sqrt{14}}$.134	.067	.045
531	$\frac{1}{\sqrt{35}}$.168	.084	.056
731	$\frac{1}{\sqrt{59}}$.130	.065	.043
751	$\frac{1}{\sqrt{75}}$.115	.058	.038
753	$\frac{1}{\sqrt{83}}$.110	.055	.037

cube. The table contains all planes having values of d/n greater than 0.12. These values are collected in Table III., arranged in order of decreasing d/n .

For convenience of reference, the spacings, *i. e.*, the distance between consecutive parallel planes of the most important forms in the four most common cubic lattices are tabulated in Table III., together with such submultiples, d/n , of these spacings as come within the range of the tables. The order is that of decreasing d/n , and the table contains all values of d/n greater than .12.¹ The table also contains the number of different sets of planes in each of the given forms. For example, the hexahedral form (100) consists of three families of parallel planes, parallel respectively to 100, 010, and 001.

To test whether any new crystal belongs to one of the lattices represented in Table III., it is only necessary to calculate the values of d/n from the lines of its powder photograph, tabulate them in order, and compare this table with Table III.

The unit of d/n in Table III. is the "lattice constant," *i. e.*, the side of the elementary cube whose successive translations can generate the whole lattice. To find the spacing of any set of planes in a crystal having one of these lattices it is only necessary to multiply the value of d given in the table by the "lattice constant" of the given crystal.

The first three lattices in the table are the regular cubic space lattices, in which every atom is equivalent in position to every other. In all other possible cubic lattices the atoms must be divided into two or more classes, whose positions in the lattice are not equivalent. The first lattice is the *simple cubic lattice*, the unit of whose structure is a cube with atoms at each corner. The positions of the atoms are specified by giving to each of the coördinates m, n, p all possible integral values within the limits of the size of the crystal. Each atom in the lattice has as nearest neighbors six symmetrically placed atoms, which form an octahedron about it. This arrangement of atoms is exemplified by rock salt, except that in rock salt the atoms are alternately sodium and chlorine. No elementary substance with simple cubic structure has yet been found.

The second lattice is a *centered cubic lattice*, whose unit is a cube with an atom in each corner, and one at the center of the cube. It may be formed by superimposing two simple cubic lattices in such manner that the atoms of the one are at the centers of the cubes of the other. The coördinates of the atoms are therefore given by $\left\{ \begin{array}{l} m, n, p \\ m + \frac{1}{2}, n + \frac{1}{2}, p + \frac{1}{2} \end{array} \right.$, where

¹ In order to shorten the table the simple cube spacings, which are much more numerous than the others, have not been tabulated beyond $d/n = .1766$.

TABLE III.

Indices of Form.	Plane Families Belonging to Form.	Spacing of Planes, Including Submultiple d/n .			
		Simple Cube.	Centered Cube.	Face-centered Cube.	Diamond.
100	3	1.00			
110	6	.707	.707		
111	4	.577		.577	.577
100	3	($n = 2$) .500	.500	.500	
210	12	.447			
211	12	.408	.408		
110	6	($n = 2$) .354	($n = 2$) .354	.354	.354
{ 221	{ 12	.3333			
{ 100	{ 3	($n = 3$) .3333			
310	12	.3160	.3160		
311	12	.3014		.301	.301
111	4	($n = 2$) .2885	.2885	($n = 2$) .2885	($n = 2$) .2885
320	12	.2774			
321	24	.2672	.2672		
100	3	($n = 4$) .2500	($n = 2$) .2500	($n = 2$) .2500	.2500
{ 410	{ 12	.2423			
{ 322	{ 12	.2423			
{ 411	{ 12	.2358	.2358		
{ 110	{ 6	($n = 3$) .2358	($n = 3$) .2358		
331	12	.2292		.2292	.2292
210	12	($n = 2$) .2234	.2234	.2234	
421	24	.2180			
332	12	.2132	.2132		
211	12	($n = 2$) .2040	($n = 2$) .2040	.2040	.2040
{ 430	{ 12	.200			
{ 100	{ 3	($n = 5$) .200			
{ 431	{ 24	.1960	.1960		
{ 510	{ 12	.1960	.1960		
{ 511	{ 12	.1923		.1923	.1923
{ 111	{ 4	($n = 3$) .1923		($n = 3$) .1923	($n = 3$) .1923
{ 520	{ 12	.1856			
{ 432	{ 24	.1856			
521	24	.1826	.1826		
110	6	($n = 4$) .1766	($n = 4$) .1766	($n = 2$) .1766	($n = 2$) .1766
{ 530	{ 12	.1714	.1714		
{ 433	{ 12	.1714	.1714		
531	24			.169	.169
{ 100	{ 3		($n = 3$) .167	($n = 3$) .167	
{ 221	{ 12		.167	.167	
{ 611	{ 12		.1621		
{ 532	{ 24		.1621		
310	12		($n = 2$) .1580	.1580	.1580
533	12			.1525	.1525
311	12		.1507	($n = 2$) .1507	($n = 2$) .1507
631	24		.1474		
111	4		($n = 2$) .1442	($n = 4$) .1442	($n = 4$) .1442

Indices of Form.	Plane Families Belonging to Form.	Spacing of Planes, Including Submultiple d/n .			
		Simple Cube.	Centered Cube.	Face-centered Cube.	Diamond.
{ 110 710 543	6		$(n = 5)$.1414 } .1414 } .1414 }		
	12				
	24				
{ 711 551	12			.1400 } .1400 }	.1400 } .1400 }
	12				
320	12		.1387	.1387	
{ 211 552 721	12		$(n = 3)$.1360 } .1360 } .1360 }		
	12				
	24				
321	24		$(n = 2)$.1336	.1336	.1336
730	12		.1312		
{ 553 731	12			.1301 } .1301 }	.1301 } .1301 }
	24				
{ 732 651	24		.1270 } .1270 }		
100	3		$(n = 4)$.1250	$(n = 4)$.1250	$(n = 2)$.1250
{ 741 811 554	24		.1230 } .1230 }		
	12		.1230 }		
	12		.1230 }		
733	12			.1222	.1222
{ 410 322	12		.1212 } .1212 }	.1212 } .1212 }	
	12		.1212 }	.1212 }	

m , n , and p have all possible integral values. Each atom in this lattice has eight equidistant nearest neighbors, which form a cube about it. Examples of this structure are iron and sodium.

The third lattice is the *face-centered cubic lattice*. Its unit of structure is a cube with an atom at each corner and one in the center of each face. It may be formed by the superposition of four simple cubic lattices with construction points¹ $0, 0, 0$; $\frac{1}{2}, \frac{1}{2}, 0$; $\frac{1}{2}, 0, \frac{1}{2}$; $0, \frac{1}{2}, \frac{1}{2}$ respectively. The coordinates of the atoms are therefore

$$\begin{aligned}
 & m, n, p, \\
 & m + \frac{1}{2}, n + \frac{1}{2}, p, \\
 & m + \frac{1}{2}, n, p + \frac{1}{2}, \\
 & m, n + \frac{1}{2}, p + \frac{1}{2},
 \end{aligned}$$

where m , n , and p have all possible integral values. Each atom in this lattice is surrounded by twelve equidistant atoms which form a regular dodecahedron about it. Examples of this structure are aluminium, copper, silver, gold and lead.

¹ The term "construction point" is used to denote the position of some definite point, which may be looked upon as the starting point (aufpunkt) of each lattice, with respect to the coordinate axes.

The fourth lattice is known as the *diamond type* of lattice, and is exemplified by diamond and silicon. It may be formed by the superposition of two face-centered lattices, with construction points 0, 0, 0, and $\frac{1}{4}, \frac{1}{4}, \frac{1}{4}$ respectively. The coördinates of the atoms are therefore

$$\begin{aligned} m, n, p, \\ m + \frac{1}{2}, n + \frac{1}{2}, p, \\ m + \frac{1}{2}, n, p + \frac{1}{2}, \\ m, n + \frac{1}{2}, p + \frac{1}{2}, \\ m + \frac{1}{4}, n + \frac{1}{4}, p + \frac{1}{4}, \\ m + \frac{3}{4}, n + \frac{3}{4}, p + \frac{1}{4}, \\ m + \frac{3}{4}, n + \frac{1}{4}, p + \frac{3}{4}, \\ m + \frac{1}{4}, n + \frac{3}{4}, p + \frac{3}{4}, \end{aligned}$$

where m , n , and p have all possible integral values.

Each atom in this lattice is surrounded by four equidistant atoms, which form a tetrahedron about it. The tetrahedra, however, are not all similarly situated, half of the atoms being surrounded by positive tetrahedra, and the other half by negative tetrahedra. In this lattice successive parallel planes are not all equidistant. In those forms whose indices are all odd numbers, as (751), (533), the planes are arranged in regularly spaced pairs, the distance between members of a pair being one fourth the distance between consecutive pairs. In all other forms, that is, those whose indices are not all odd, the spacing is regular.

B. Crystals Other Than Cubic.

In the case of crystals belonging to systems other than the cubic, the procedure is not so simple. It is necessary to make a separate calculation, not only for every kind of atomic grouping, but for every different ratio of the axes or angle between axes. When these axes are not known from crystallographic data, as in the case of graphite, for example, a great many trials have to be made before the correct one is found. Also, in the case of oblique axes the formula for the distance between planes is less simple. However, when the crystallographic data is reliable the process is not difficult. A few examples will be given below for illustration and reference.

The general formula for the distance from a plane h, k, l (Miller indices) to a parallel plane through the point x_1, y_1, z_1 , referred to any system of

axes X, Y, Z , having angles λ, μ, ν between the axes YZ, XZ , and XY respectively, is¹

$$d = \frac{hx_1 + ky_1 + lz_1 - 1}{\left[\begin{array}{c|c|c} \hline h \cos \nu \cos \mu & 1 & h \cos \mu \\ \hline h & k & 1 \\ \hline l \cos \lambda & 1 & \\ \hline \end{array} \right]^{1/2} + \left[\begin{array}{c|c|c} \hline \cos \lambda & \cos \nu & k \cos \lambda \\ \hline k & \cos \nu & k \\ \hline 1 & \cos \mu & l \\ \hline \end{array} \right]^{1/2} + \left[\begin{array}{c|c|c} \hline 1 & \cos \nu & h \\ \hline \cos \nu & 1 & k \\ \hline \cos \mu & \cos \lambda & l \\ \hline \end{array} \right]^{1/2}} \quad (2)$$

For the three rectangular systems, the cubic, tetragonal and orthorhombic, λ, μ , and ν are each 90° and equation (2) reduces to equation (1). For the tetragonal and orthorhombic systems, however, and in all the other systems except the cubic and trigonal, the coördinates x_1, y_1, z_1 , and the indices h, k , and l are not all measured in the same units. The products hx_1, ky_1, lz_1 , of the numerator are of zero dimensions, but the values of h, k , and l in the denominator contain the units, and must be replaced by $h/a, k/b, l/c$, where a, b , and c are the unit axes of the crystal in the X, Y , and Z directions respectively. This gives:

For the tetragonal system

$$d = \frac{hx_1 + ky_1 + lz_1 - 1}{\sqrt{h^2 + k^2 + (l/c)^2}}, \quad (3)$$

where c is the axial ratio of the crystal; and for the orthorhombic system

$$d = \frac{hx_1 + ky_1 + lz_1 - 1}{\sqrt{(h/a)^2 + k^2 + (l/c)^2}}, \quad (4)$$

where a and c are the lengths of the shorter lateral axis and vertical axis respectively.

For the hexagonal system, if two of the horizontal axes, 120° apart, are taken as X and Y , and the vertical axis as Z , λ and μ are each 90° and ν 120° , and equation (2) reduces to

¹ This formula is easily obtained from the fundamental equation

$$d = x_1 \cos \alpha + y_1 \cos \beta + z_1 \cos \gamma - p,$$

by substituting for $\cos \alpha, \cos \beta, \cos \gamma$, and p their values in terms of h, k, l, λ, μ , and ν given by the equations:

$$\begin{aligned} \cos \alpha &= l' + m \cos \nu + n \cos \mu = hp \\ \cos \beta &= l' \cos \nu + m + n \cos \lambda = kp \\ \cos \gamma &= l' \cos \mu + m \cos \lambda + n = lp \\ l' \cos \alpha + m \cos \beta + n \cos \gamma &= 1 \end{aligned}$$

where $\cos \alpha, \cos \beta, \cos \gamma$ are the direction cosines, and l', m, n the direction ratios of the perpendicular p from the origin to the plane hkl .

$$d = \frac{hx_1 + ky_1 + lz_1 - 1}{\sqrt{4/3(h^2 + hk + k^2) + (l/c)^2}}, \quad (5)$$

where c is the "axial ratio" for the particular crystal species.

For the trigonal system, in which $\lambda = \mu = \nu$, equation 2 reduces to

$$d = \frac{(hx_1 + ky_1 + lz_1 - 1)\sqrt{1 + 2 \cos^3 \lambda - 3 \cos^2 \lambda}}{\sqrt{(h^2 + k^2 + l^2) \sin^2 \lambda + 2(hk + hl + kl)(\cos^2 \lambda - \cos \lambda)}}. \quad (6)$$

For the monoclinic system λ and ν are each 90° and equation (2) becomes

$$d = \frac{hx_1 + ky_1 + lz_1 - 1}{\sqrt{\frac{\left(\frac{h}{a}\right)^2 + \left(\frac{l}{c}\right)^2 - 2\frac{hl}{ac} \cos \mu}{\sin^2 \mu} + k^2}}, \quad (7)$$

where a and c refer to the lengths of the clinodiagonal and vertical axes respectively, the orthodiagonal axis b being taken as unity.

Finally, for the triclinic system, for which the general equation (2) must be used, it should be noted that in order to use the equation for numerical calculation, the quantities h , k , and l in the denominator should be divided by the corresponding axial lengths a , b , c .

Standard tables of calculated spacings, like Table III. above, cannot be given for crystal systems other than the isometric, since the axial ratios and angles are different for each crystal. By way of example, however, the spacings of three hexagonal lattices having the axial ratio 1.624, which is the accepted value for magnesium, are given in Table IV. The first is a simple lattice of triangular prisms, the length of whose side is taken as unity and whose height is therefore 1.624. It is one of the regular space lattices. The positions of the atoms in this lattice are given, in hexagonal coordinates (see equation (5) above) by $(x, y, z) = m, n, pc$ where each of the coordinates m , n , and p assumes all possible integral values, and c is the axial ratio. The second lattice in Table IV. is composed of two of the above triangular lattices intermeshed in such a way that the atoms of the first are in the centers of the prisms of the second and vice versa. It differs but very little from the so-called hexagonal close-packing, which is one of the two alternative arrangements which the atoms would assume if they were hard spheres and were forced by pressure into the closest possible packing. The positions of the atoms are given by $\begin{cases} m, n, pc \\ m + \frac{1}{3}, n + \frac{2}{3}, (p + \frac{1}{2})c \end{cases}$ where the coordinates refer to hexagonal axes, and m, n, p , have all possible integral values. The third lattice in Table IV. is composed of three of the above simple triangular

lattices, the atoms of the second and third being directly above the centers of the alternate triangles of the first lattice, at distances of $\frac{1}{3}$ and $\frac{2}{3}$ respectively of the height of the prism. It is the regular rhombohedral lattice. The positions of the atoms in this lattice may be most simply specified with reference to trigonal axes, but for convenience of comparison with the first two lattices, they are given in terms of hexagonal axes. Their hexagonal coordinates are

$$\left\{ \begin{array}{l} m, \quad n, \quad pc, \\ m + \frac{1}{3}, n + \frac{2}{3}, (p + \frac{1}{3})c \\ m + \frac{2}{3}, n + \frac{1}{3}, (p + \frac{2}{3})c \end{array} \right\}.$$

where m , n , and p have all possible integral values, and c is the axial ratio 1.624.

The first column in Table IV. gives the indices of the form, the second,

TABLE IV.

Indices of Form.	Simple Triangular Lattice.		Close-packed Lattice.		Rhombohedral Lattice.		
	Number of Co-operating Planes.	Spacing of Planes.	Number of Co-operating Planes.	Spacing of Planes.	Number of Co-operating Planes.	Spacing of Planes.	Trigonal Indices of Form.
0001	1	1.624					
1010	3	.866	3	.866			
0001	1	($n = 2$) .812	1	.812			
1011	6	.764	6	.764	3	.764	100
1012	6	.592	6	.592	3	.592	110
0001	1	($n = 3$) .541			1	.541	111
1120	3	.500	3	.500	3	.500	$\bar{1}10$
1121	6	.477					
1013	6	.458	6	.458			
1010	3	($n = 2$) .433	3	($n = 2$) .433			
1122	6	.426	6	.426			
2021	6	.418	6	.418	3	.418	$\bar{1}11$
0001	1	($n = 4$) .406	1	($n = 2$) .406			
1011	6	($n = 2$) .382	6	($n = 2$) .382	3	($n = 2$) .382	100
1014	6	.368	6	.368	3	.368	211
1123	6	.367			6	.367	210
2023	6	.338	6	.338			
2130	6	.327	6	.327			
0001	1	($n = 5$) .325					
2131	12	.321	12	.321	6	.321	$\bar{2}10$
1124	6	.315	6	.315			
{ 1015	6	.304	6	.304	3	.304	221
	12	.304	12	.304	6	.304	$\bar{2}\bar{1}1$
1012	6	($n = 2$) .296	6	($n = 2$) .296	3	($n = 2$) .296	110
1010	3	($n = 3$) .289	3	($n = 3$) .289	3	.289	$\bar{2}11$

fourth and sixth the number of different families of planes belonging to the form, and the third, fifth and seventh the spacing of these planes in the respective lattices, found by substituting the coördinates of the atoms in equation (5). The unit is the side of the elementary triangular prism. The eighth column gives, for comparison, the indices of the planes of the rhombohedral lattice in trigonal (Miller) coördinates. The atoms are in this case referred to three equal axes, making equal angles of 78.4° with each other, and their coördinates are m, n, p , where each of these numbers has all possible integral values.

Examples.

As examples of the application of the method of analysis described above, the analysis of ten elementary crystalline substances is given below. Three of these analyses are incomplete, but are of such importance as to warrant their inclusion. Four others have already been briefly described elsewhere, and are given here in more detail. The last, diamond, which has been completely analyzed by the Braggs, is added as a check upon the method, and as an example of the immense amount of information which can be obtained from a single photograph.

The experimental data is collected in Tables V. to XIV. The first column in each table gives the estimated intensity of each line. The estimate is necessarily very rough, but photometric measurements have little value unless care is taken to make control exposures to determine the characteristic curve of the plate under the actual conditions of exposure and development. In the photographs here described, this was not done. The second column gives the distance, x , of each line on the photograph from the central undeviated image of the slit. The third column gives the angular deviation 2θ , of the ray that produced the line, calculated from x and the distance between crystalline material and photographic plate. The fourth and fifth columns give the experimental and theoretical values of d/n , where d is the distance in Ångstroms between consecutive planes, and n the order of reflection. The experimental values of d/n are calculated from the angular deviation 2θ by means of the equation $n\lambda = 2d \sin \theta$. The theoretical values are obtained by multiplying the values in Tables III. and IV. by the lattice constants of the respective crystals. The sixth column gives the indices of the forms to which the reflecting planes belong, and the last column the number of families of planes belonging to the given form and having the same spacing, so that their reflections are superimposed. The number of these coöperating planes is a measure of the intensity of the line to be expected if the atoms are symmetrical and equally distributed in successive planes.

IRON.

The iron investigated was obtained from two sources, viz., fine filings of pure electrolytic iron, and fine iron powder obtained by the reduction of Fe_2O_3 in hydrogen. The filings were mounted in a thin-walled glass tube 2 mm. in diameter, which was kept in rotation during the exposure. The reduced oxide was pressed into a sheet 2 mm. thick, which was mounted firmly at right angles to the beam of X-rays. Both specimens gave the same lines.

A fine-focus Coolidge X-ray tube with tungsten target was used for all the iron photographs. It was operated by the constant potential equipment which has been in use for two years in the Research Laboratory,¹ at 110,000 volts and 1 milliamperere.

Fig. 6 shows one of the photographs of the iron powder (reduced oxide). For all lines beyond the first three, the α doublet is resolved into two very narrow, sharp lines. The β line of the K radiation is visible on the plate for some of the stronger reflections, but is easily distinguishable from the double α line. In this exposure both slits were very narrow, about 0.2 mm. wide. The distance from X-ray tube to first slit was 20 cm., from first to second slit 15 cm., and from crystal to photographic plate 18.15 cm. Seed X-ray plate was used, with calcium tungstate intensifying screen. The exposure was 20 hours.

The lines in this photograph are tabulated in Table V., together with the calculated spacings, as described above. The observed spacings (column 4) agree with the theoretical spacings for a centered cube of side 2.86 Å. (column 5) within the limit of accuracy of measurement of the lines. The intensities also vary in the manner to be expected, except that the second order 110 line is too intense and the second order 100 too weak. The bearing of this fact on the question of the arrangement of electrons in the iron atom has been discussed elsewhere.²

A centered cubic lattice should have two atoms associated with each elementary cube. By equating the mass of the n atoms in an elementary cube to the mass of the cube, *i. e.*, its volume \times density of the metal, we obtain

$$n = \frac{\rho d^3}{M} = \frac{7.86 \times 2.86^3 \times 10^{-24}}{55.4 \times 1.663 \times 10^{-24}} = 2.00.$$

As a check upon this analysis, photographs were taken of single crystals of silicon steel, containing about 3.5 per cent. silicon, which were mounted on the spectrometer table and rotated about definite axes. Two of these photographs are reproduced in Fig. 7. The first,

¹ PHYS. REV., 7, 405, 1916. For a fuller description see G. E. Review, 19, 173, March, 1916.

² PHYS. REV., 9, 84, 1917.

TABLE V.

Iron.

Intensity of Line.	Distance of Line from Center.	Angular Deviation of Line θ .	Spacing of Planes in Ångstroms.		Indices of Form.	Number of Cooperating Planes.
			Experimental.	Theoretical.		
1.00	1.87	5.90	2.05	2.06	110	6
.46	2.67	8.40	1.43	1.43	100	3
.54	3.40	10.30	1.16	1.16	211	12
.24	3.85	11.96	1.005	1.01	110 ($n = 2$)	3
.18	4.32	13.40	.910	.905	310	12
.16	4.75	14.67	.823	.826	111	4
.22	5.17	15.90	.757	.765	321	24
				.715	100 ($n = 2$)	3
.12	5.92	18.06	.665	.675	{ 110 ($n = 3$) 411	18
.03	6.27	19.06	.633	.638	210	12
.02	6.62	20.06	.600	.610	332	12
.02	7.00	21.10	.572	.584	211 ($n = 2$)	12
.10	7.25	21.78	.555	.560	{ 510 431	36
.02	7.95	23.16	.522	.522	521	24

Fig. 7a, is the photograph of a thin crystal about 5 mm. square, cut parallel to 100. It was mounted 12 cm. from the photographic plate, with its 100 face normal to a beam of tungsten rays, and rotated slowly, about an axis perpendicular to 001, for a few degrees on each side of the center. It shows, in the horizontal plane, the spectrum of the tungsten target reflected from 010, and at 45° and 135° the same reflected from 011 and $0\bar{1}1$ respectively. The two K lines in tungsten, the unresolved α doublet and the β line, show plainly in each of these spectra, and the distance between the α doublets of the right and left spectra, viz., 3.56 cm. for 010, and 2.50 cm. for 011, give for the spacings of these planes

$$d_{010} = 1.43 \text{ \AA.},$$

$$d_{011} = 2.04 \text{ \AA.}$$

The second photograph, Fig. 7b, shows the result of rotating a thin crystal cut parallel to 111, and mounted normal to the rays, about an axis perpendicular to 110, for a few degrees on each side. It shows, in the horizontal plane, the reflection from $\bar{1}\bar{1}2$, and at 30° , 60° and 71° , to the horizontal the reflections from $\bar{1}01$, $\bar{2}11$, $\bar{3}21$, with corresponding reflection from $2\bar{3}1$, 121 and $0\bar{1}1$ at angles of 109° , 120° and 150° respectively to the horizontal. The planes $\bar{1}01$ and $0\bar{1}1$ show both first and second order spectra. The distances between α lines of these spectra

agree excellently for planes belonging to the same form, and give for the spacing of the planes in the three forms represented:

$$\begin{aligned}d_{211} &= 1.15 \text{ \AA.}, \\d_{110} &= 2.02 \text{ \AA.}, \\d_{321} &= 0.75 \text{ \AA.}\end{aligned}$$

The agreement of these angles and spacings with the theoretical values for a centered cubic lattice indicates that the position of the atoms in iron is not greatly affected by the presence of $3\frac{1}{2}$ per cent. Si.

A series of photographs of one of these crystals at liquid air temperature, room temperature, and 1000°C. respectively showed no observable change, even in intensities. It is necessary to photograph more forms, however, before definite conclusions can be drawn regarding the relation of α to β iron. Several photographs of iron powder at different temperatures between 700°C. and 900°C. were spoiled, either by chemical fog due to the heating of the photographic plate, or by the growth of the crystals during exposure, thus giving only a few large spots on the photograph.

SILICON.

Small crystals of metallic silicon were crushed in a mortar and sifted through a gauge of 200 meshes to the inch. The fine powder was mounted in a very thin-walled tube of lime glass, and kept in continuous rotation during a four hour exposure to rays from a molybdenum target, running at 32 k.v. constant potential and 8 milliamperes. A filter of zircon powder .037 cm. thick reduced the spectrum essentially to a single line, the unresolved α doublet, $\lambda = .712$, of molybdenum, as shown in Fig. 3. The crystal was 15 cm. from the X-ray target and 11.3 cm. from the photographic film, which was bent in the arc of a circle, with the crystal at the center. Both slits were quite wide, about 1 mm., and about 5 cm. apart. Eastman X-ray film was used, with calcium tungstate intensifying screen.

The photograph obtained is reproduced in Fig. 8, and the measurements are given in Table VI. The spacings tabulated as "theoretical" are those of a lattice of the diamond type, *i. e.*, two intermeshed face-centered lattices, each of side 5.43 Å., one lattice being displaced, with reference to the other, along the cube diagonal a distance one fourth the length of the diagonal. The agreement is perfect. The estimates of intensity are not accurate enough to warrant discussion.

The number of atoms associated with each unit cube is

$$n = \frac{\rho d^3}{M} = \frac{2.34 \times 5.43^3}{28.1 \times 1.663} = 8.00,$$

which is the correct number for this type of lattice.

TABLE VI.
Silicon.

Intensity of Line.	Distance of Line from Center.	Angular Deviation of Line θ .	Spacing of Planes in Ångströms.		Indices of Form.	Number of Cooperating Planes.
			Experimental.	Theoretical.		
1.00	2.58	13.56	3.13	3.14	111	4
.80	4.21	23.0	1.93	1.93	110	6
.75	4.97	26.16	1.64	1.64	311	12
0				1.57	111 ($n=2$)	4
.25	6.00	31.58	1.36	1.356	100	3
.45	6.54	34.42	1.25	1.25	331	12
.50	7.39	38.92	1.11	1.11	211	12
.40	7.84	40.78	1.05	1.04	{ 511 111 ($n=3$)	16
.20	8.59	45.20	.96	.96	110 ($n=2$)	6
.30	8.98	47.22	.92	.92	531	24
.25	9.66	50.44	.86	.86	310	12
.10	10.01	52.44	.83	.83	533	12
0				.82	311 ($n=2$)	12
.05	10.62	55.70	.79	.79	111 ($n=4$)	4
.10	11.00	59.76	.76	.76	{ 711 551	24
.20	11.58	60.36	.73	.73	321	24
.15	11.90	62.56	.71	.71	{ 731 553	36
0				.68	100 ($n=2$)	3
0				.66	733	12
.05	13.33	70.0	.64	.64	411	12
.05	13.60	71.44	.63	.63	{ 751 111 ($n=5$)	28

ALUMINIUM.

Fine filings of pure sheet aluminium were mounted in exactly the same manner as silicon, and exposed for 3 hours to molybdenum rays, produced at 40,000 volts, 9 milliamperes, and filtered by .037 cm. of zircon powder. The photograph obtained is shown in Fig. 9, and the measurements are given in Table VII.

The "theoretical" spacings in Table VII. are those of a face-centered cubic lattice. Their agreement with the "experimental" values obtained from the lines on the photograph is satisfactory.

The number of atoms per unit elementary cube is

$$n = \frac{\rho d^3}{M} = \frac{2.70 \times (4.05)^3}{2.69 \times 1.663} = 4.00.$$

This is the correct number for a face-centered lattice.

TABLE VII.

Aluminium.

Intensity of Line.	Distance of Line from Center.	Angular Deviation of Line 2θ .	Spacing of Planes in Ångstroms.		Indices of Form.	Number of Coöperating Planes.
			Experimental.	Theoretical.		
Estimated.	Cm.	Degrees.				
1.00	3.45	17.80	2.33	2.33	111	4
.60	3.99	20.60	2.025	2.025	100	3
.50	5.67	29.26	1.43	1.43	110	6
.60	6.68	34.5	1.21	1.22	311	12
.20	6.95	35.8	1.17	1.17	111 ($n = 2$)	4
.05	8.09	41.8	1.01	1.01	100 ($n = 2$)	3
.25	8.86	45.6	.93	.93	331	12
.25	9.11	47.0	.90	.90	210	12
.10	10.05	51.8	.82	.83	211	12
.15	10.66	55.0	.78	.78	{ 511	
					{ 111 ($n = 3$)	16
.02	11.75	60.6	.71	.72	110 ($n = 2$)	6
.04	12.30	63.4	.68	.68	531	24

The unit of structure of the aluminium crystal is, therefore, a face-centered cube, of side 4.05 Å., with one atom of aluminium at each corner and one at the center of each face.

MAGNESIUM.

The magnesium used in these experiments was the commercial electrolytic product made in the research laboratory. Several photographs were taken, some with fine filings from cast rods of this metal, and some with filings from large crystals formed by vacuum distillation. Both kinds of powder gave the same results.

The powder was mounted in a 2 mm. tube of thin glass, and exposed under exactly the same conditions as silicon and aluminium. Fig. 10 shows a photograph obtained from a 6-hour exposure at 32,000 volts and 9 milliamperes, and Table VIII. gives the numerical data.

The "theoretical spacings" in Table VIII. are those of a hexagonal lattice composed of two sets of triangular prisms, each of side 3.22 Å. and axial ratio 1.624, with construction points 000 and $\frac{1}{3}$, $\frac{2}{3}$, $\frac{1}{2}$ respectively. This is the lattice whose spacings are given in column 5 of Table IV., under "Close-Packed Lattice." It is slightly distorted, however, from true hexagonal close packing, which requires an axial ratio of 1.633. This variation from theoretical close packing is to be attributed to a slight asymmetry in the structure of the magnesium atoms.

The agreement between calculated and experimental spacings is satisfactory, except that several lines which were to be expected do not

show in the photograph. In particular, the reflection from the basal plane, 0001, is absent in all the photographs.

It seemed desirable, therefore, to supplement the evidence furnished by the powder photographs by photographs of single crystals, mounted

TABLE VIII.
Magnesium.

Intensity of Line.	Distance of Line from Center.	Angle of Reflection.	Spacing of Planes in Angstroms.		Indices of Form.	Number of Cooperating Planes.
			Experimental.	Theoretical.		
.40	2.92	14.80	2.75	2.75	10 $\bar{1}$ 0	3
				2.59	0001	1
1.00	3.30	16.66	2.44	2.44	10 $\bar{1}$ 1	6
.30	4.23	21.48	1.91	1.90	10 $\bar{1}$ 2	6
.40	5.03	25.50	1.61	1.60	11 $\bar{2}$ 0	3
.35	5.50	27.8	1.48	1.48	10 $\bar{1}$ 3	6
				1.38	10 $\bar{1}$ 0(2)	3
.35	5.95	30.0	1.36	1.36	11 $\bar{3}$ 2	6
.12	6.05	30.6	1.34	1.34	20 $\bar{2}$ 1	6
				1.30	0001(2)	1
.06	6.65	33.6	1.23	1.23	10 $\bar{1}$ 1(2)	6
.02	6.9	34.8	1.18	1.18	10 $\bar{1}$ 4	6
.10	7.52	38.0	1.09	1.08	20 $\bar{2}$ 3	6
.18	7.96	40.2	1.04	1.05	21 $\bar{3}$ 0	6
.02	8.1	41.0	1.02	1.03	21 $\bar{3}$ 1	12
				1.01	11 $\bar{2}$ 4	6
.12	8.41	42.6	.98	.97	{ 21 $\bar{3}$ 2	
					{ 10 $\bar{1}$ 5	18
				.94	10 $\bar{1}$ 2(2)	6
.01	8.83	44.8	.93	.92	10 $\bar{1}$ 0(3)	3
.10	9.15	46.2	.90	.89	21 $\bar{3}$ 3	12
.06	9.48	48.0	.87	.87	{ 30 $\bar{3}$ 2	
					{ 0001(3)	7
.02	9.90	50.2	.83	.83	{ 10 $\bar{1}$ 6	
					{ 20 $\bar{2}$ 5	12
				.82	{ 10 $\bar{1}$ 1(3)	
					{ 21 $\bar{3}$ 4	18
				.80	11 $\bar{2}$ 0(2)	3
.06	10.95	55.4	.77	.77	31 $\bar{4}$ 0	6

with definite orientations. Several such photographs were taken, the measurements of three of which are given in Table IX. The crystals were formed by vacuum distillation, and were about 2 mm. in diameter. The first was mounted with its basal plane (0001) parallel to the rays, and rotated slowly about an axis normal to $1\bar{2}10$, for about 30° on each side of the center.¹

¹ The reflection from $10\bar{1}0$ should not have appeared on this plate. It was very faint, but clearly visible on both sides, and was probably due to a twin upon $10\bar{1}1$, a small portion

The second crystal was mounted so as to rotate about the same axis as the first, but with $10\bar{1}0$ parallel to the rays at the start. The third was mounted with 1120 parallel to the rays, and rotated about an axis normal to 1100 . The patterns obtained in these photographs differed from those of the single iron crystals in containing reflections from many more planes, corresponding to the greater complexity of the hexagonal system. Molybdenum rays were used, filtered through .037 cm. of zircon, so that the spectrum consisted of a single line.

The lines reflected in the horizontal plane, which appeared on the three photographs, are given in Table IX. The 0001 reflection was very strong on the first photograph, and on three additional photographs which were taken to make certain its identity. Its absence in all the powder photographs must be due, therefore, to the much greater relative intensity of the reflections from other forms, containing many more planes. These forms reflect not only the lines but the unabsorbed part of the general spectrum, causing a fog over the plate that obscures weak lines.

TABLE IX.

Crystal 1.			Crystal 2.			Crystal 3.		
Position of Line.	Spacing of Plane.	Indices of Plane.	Position of Line.	Spacing of Plane.	Indices of Plane.	Position of Line.	Spacing of Plane.	Indices of Plane.
3.10	2.59	0001	2.90	2.75	$10\bar{1}0$	5.02	1.60	$11\bar{2}0$
2.90	2.75	$10\bar{1}0$	3.10	2.59	0001	5.50	1.48	$10\bar{2}1$
3.30	2.44	$10\bar{1}1$	3.30	2.44	$10\bar{1}1$	6.0	1.36	$11\bar{2}2$
4.20	1.90	$10\bar{1}2$	6.05	1.34	$20\bar{2}1$			
5.50	1.48	$10\bar{1}3$	8.92	0.92	$10\bar{1}0(3)$			
6.27	1.30	0001(2)	5.9	1.38	$10\bar{1}0(2)$			

The lines tabulated in Table IX., and all the others which appeared on these photographs, are the ones which should appear, with the exceptions mentioned in the above note.

The evidence seems sufficient that the assumed structure is correct, viz., that the atoms of magnesium are arranged on two interpenetrating lattices of triangular prisms, each of side 3.22 Å. and height 5.23 Å., with one atom at each corner, the atoms of one set being in the center of the prisms of the other.

SODIUM.

The first photographs of sodium were of rods, about 1 mm. in diameter and 1 cm. long, cut from an old sample that had been in the laboratory of which was included in cutting the crystal from the mass of other crystals upon which it grew. A second specimen mounted and photographed in the same manner did not show this line. Similar twinning must account for the 0001 reflection shown by crystal 2, and $10\bar{1}3$ by crystal 3.

several years. These rods were placed in sealed glass tubes, and exposed to molybdenum rays. They gave intense reflections, of a pattern which indicated that the lump from which the samples were cut was a single large crystal.

Several unsuccessful attempts were then made to obtain finely divided crystals of sodium. Distillation in vacuum into the thin-walled tube which was to be photographed was found impossible. Several different glasses and pure silica tubing were tried. The sodium always ate through the tube wall before it could be coaxed into the narrow tube. Melting the distilled sodium so that it flowed into the tube resulted in an amorphous condition, which gave no lines at all. It is probable that distillation, had it succeeded, would have given the same result, for potassium distilled in this way was found to be completely amorphous. Shaking in hot xylol gave a beautiful collection of tiny spheres, but these too were amorphous, and annealing for 16 hours at 90° C. failed to produce any appreciable crystallization. Crystallization from ammonia solution gave a black mass, from which it was difficult to separate the pure sodium. Fairly good photographs were obtained with fine shreds, scraped from the lump, with a knife, under dry xylol, and packed in a small glass tube.

A satisfactory sample was finally prepared by squirting the cold metal through a .01 cm. die, and packing the fine thread, with random folding, into a 1 mm. glass tube, which was immediately sealed. The sample from which this was taken was about two months old, and was apparently only slightly crystallized, so that only a few lines were visible, on the dense continuous background due to the amorphous part. Two photographs, taken under the same conditions as the preceding, with exposures of 4 and 14 hours respectively at 30 k.v. 27 milliamperes, gave identical lines, which are tabulated in Table X.

TABLE X.

Sodium.

Intensity of Line.	Distance of Line from Center.	Angular Deviation of Line θ .	Spacing of Planes in Ångstroms.		Indices of Form.	Number of Cooperating Planes.
			Experimental.	Theoretical (Centered Cube).		
Estimated.	Cm.	Degrees.				
1.00	2.66	13.38	3.05	3.04	110	6
.10	3.78	19.06	2.15	2.15	100	3
.40	4.66	23.36	1.76	1.76	211	12
.10	5.38	27.04	1.52	1.52	110(2)	6
.08	6.03	30.26	1.36	1.36	310	12
.02	6.57	33.40	1.24	1.24	111	4
.05	7.18	36.0	1.15	1.15	32	24

These seven lines, which are the only ones that appeared on any of the sodium photographs, agree perfectly with the theoretical spacings of a centered cubic lattice, of side 4.30 Å., and cannot be made to fit any other simple type of lattice.

The number of atoms per elementary cube is

$$n = \frac{0.970 \times 4.30^3}{22.8 \times 1.663} = 2.03,$$

which is as close to the required number, two, as the data would warrant.

The evidence is sufficient, I think, in spite of the limited number of lines, to show that the atoms of sodium, when in its crystalline form, are arranged on a lattice whose unit of structure is a centered cube, of side 4.30 Å., with one atom at each corner and one in the center of the cube. The tendency to form this regular arrangement is, however, very slight, corresponding to a small difference between the potential energies of the crystalline and amorphous states. This fact is important for the determination of the structure of the sodium atom.

The structures of the elements thus far described have been determined with considerable certainty. The three following have been only partially determined, but are included as examples of the possibilities, as well as the difficulties, of the analysis.

LITHIUM.

The structure of lithium is of special interest because, on account of the small number of electrons associated with each atom, it may be expected to yield valuable information regarding the arrangement of these electrons around the nucleus. The analysis is difficult, however, on account of the complete lack of crystallographic data, the slowness of crystallization, and the difficulty of obtaining pure metal.

It was first attempted to distill lithium in vacuum, for the double purpose of purification and of obtaining small crystals. Various methods of heating the metal were tried, such as a tungsten spiral with the lithium ribbon lying in its axis, a molybdenum cup heated externally by electron bombardment, etc., but without success. The metal reacts violently with glass and silica at temperatures far below those at which its vapor pressure is appreciable.

Two samples were used. The first was prepared by electrolysis of pure lithium chloride, in a graphite crucible, and probably contains little impurity except carbon. A small lump was rolled, between steel surfaces, into a cylinder 2 mm. in diameter, and sealed in a glass tube. It was exposed, in the same manner as the previous crystals, for 7 hours

to molybdenum rays at 40 k.v. and 6 milliamperes, and gave the lines tabulated in Table XI.

TABLE XI.

Lithium.

Intensity of Line.	Distance of Line from Center.	Angular Deviation of Line θ .	Spacing of Planes in Angstroms.		Indices of Form.	Number of Cooperating Planes.
			Experimental.	Theoretical (Simple Cube).		
				3.50	100	3
.70	3.20	16.50	2.50	2.48	110	6
1.00	3.96	20.44	2.02	2.02	111	4
.05	4.61	23.4	1.75	1.75	100(2)	3
				1.56	210	12
.40	5.62	29.0	1.43	1.43	211	12
.02	6.5	33.6	1.24	1.24	110(2)	6
.60	6.95	35.9	1.17	1.17	{ 221	15
					{ 100(3)	
				1.10	310	
				1.05	311	
.10	8.07	41.6	1.01	1.01	111(2)	4
				.97	320	12
				.87	100(4)	3
				.85	{ 410	24
					{ 322	
.05	9.99	51.6	.83	.83	{ 411	18
					{ 110(3)	
				.80	331	12
.20	10.82	56.0	.77	.78	210(2)	12

The spacings calculated are those of a simple cubic lattice, of side 3.50 Å., and the density of lithium requires that 2 atoms be associated with each point of the lattice, viz.:

$$n = \frac{\rho d^3}{M} = \frac{0.53 \times 3.50^3}{6.89 \times 1.663} = 2.00.$$

A centered cubic lattice in which half of the atoms, those belonging to one of the two component simple cubic lattices, are oriented oppositely to the other half, could probably be made to fit the observations by assuming a suitable arrangement of the electrons in the atoms. It is more probable, however, in view of the next photograph, that the strong lines at 3.96 cm. and 6.95 cm. are due either to an impurity or to the admixture of a second form of lithium. All the other lines in Table XI. are consistent with a centered cubic lattice, of side 3.50 Å., with one atom of lithium at each cube corner and one in the center of each cube.

The second sample was taken from a very old stock of supposedly very pure lithium, origin not known. A fine thread was squirted through a die and packed into a glass tube, in the same manner as sodium. A five-hour exposure to molybdenum rays, at 30 k.v. 27 milliamperes, gave only 3 lines, viz., a strong line at 3.22 cm., and two weaker lines at 4.60 cm., and 5.46 cm. These are exactly the positions of the first three lines of the centered cubic lattice described above, and it is especially noteworthy that the line at 4.60 is relatively much stronger than on the preceding photograph, and the *strong lines at 3.96 cm. and 6.95 cm. are entirely lacking*. One is tempted to consider this last photograph as that of pure lithium, since its interpretation is simpler than the preceding, and it gives to lithium the same structure as sodium. The number of lines is too small, however, to justify this conclusion, and further experiments with purer metal are needed.

NICKEL.

Specially purified nickel wire was melted in vacuum and cast in a lump. Filings from this lump were placed in a small cell 2.5 mm. thick, and exposed 4 hours to tungsten rays, produced at 110,000 volts, 1 milliampere, filtered through .015 cm. of tantalum. The photographic plate was placed 15.7 cm. from the crystal, at right angles to the beam of X-rays. The lines obtained are tabulated in Table XII.

TABLE XII.

Nickel.

Intensity of Line.	Distance of Line from Center.	Angular Deviation of Line θ .	Spacing of Planes in Ångstroms.		Indices of Form.	Number of Cooperating Planes.
			Experimental.	Theoretical (Centered Cube).		
Estimated.	Cm.	Degrees.				
Very strong....	1.70	6.17	1.95	1.95	110	6
Faint.....	2.42	8.75	1.38	1.38	100	3
Strong.....	2.97	10.70	1.13	1.13	211	12
Medium.....	3.42	12.25	.98	.98	110(2)	6
Faint.....	3.80	13.60	.89	.87	310	12
				.79	111	4
Strong.....	4.58	16.28	.74	.74	321	24

The spacings agree perfectly with those of a centered cubic lattice, of side 2.76 Å., with one atom of nickel at each cube corner and one in the center of the cube. Taking the density of pure nickel as 9.00, which is probably too low, the number of atoms associated with each elementary cube is

$$n = \frac{\rho d^3}{M} = \frac{9.00 \times 2.76^3}{58.2 \times 1.663} = 1.95,$$

which is as close to the required value, 2, as the data will warrant.

Three other photographs, one of a thick electrolytic deposit on very thin nickel foil, the other two of a 2 mm. nickel rod of unknown origin, gave quite different lines. The electrolytic deposit was exposed but a short time, and gave 4 lines, at 1.64, 1.89, 2.70 and 3.14 cm. corresponding to spacings of 2.01, 1.76, 1.25, 1.07 respectively, *which are exactly the spacings of the first four lines of a face-centered cube, of side 3.52 Å.* The number of atoms associated with the elementary cube is

$$\frac{9 \times 3.52^3}{58.2 \times 1.663} = 4.02,$$

which is correct for a face-centered cubic lattice containing one atom of nickel at each cube corner and one in the center of each face.

The other two photographs, of the nickel rod of unknown origin, contained the lines of both the preceding ones, but only these lines. It was presumably a mixture of the two crystalline forms of nickel, represented by the two preceding specimens respectively.

The evidence is very strong, therefore, that nickel crystallizes in two different forms, one a centered cubic lattice, like iron, and the other a face-centered cubic lattice, like copper. The relation of the magnetic and mechanical properties to these crystalline changes has not been studied, and the above analysis is to be regarded as only preliminary.

GRAPHITE.

Several photographs of both natural and artificial graphite have been taken. The natural graphite was in large flakes, obtained from the Dixon Crucible Company. The artificial graphite was a very fine powder, furnished by the Acheson Company. Both had been heated to 3500° C. in a special graphite furnace to remove impurities and ash.

The natural graphite, either in large flakes or where pressed into a glass tube, gave very unsymmetrical photographs, showing the predominance of certain orientations of the crystals. By forcing it through a copper gauze of 100 meshes to the inch, a powder was obtained which, when packed in a glass tube and kept in rotation, gave very regular and symmetrical photographs. *The lines in these photographs were identical with those in the photographs of artificial graphite,* showing that the two are identical in crystalline structure. One of these photographs, obtained from a 16-hour exposure to Mo rays at 34,000 volts and 16 milliamperes, is reproduced in Fig. 11, and the lines, together with the calculated spacings, are tabulated in Table XIII.

TABLE XIII.

Graphite.

Intensity of Line.	Distance of Line from Center.	Angular Deviation of Line.	Spacing of Planes in Angstroms.		Indices of Form.	Number of Cooperating Planes.
			Estimated.	Theoretical.		
100	2.40	12.16	3.37	3.37	0001	1
30	3.84	19.46	2.11	2.12	10 $\bar{1}$ 0	3
60	3.99	20.20	2.03	2.02	10 $\bar{1}$ 1	6
1	4.47	22.60	1.81	1.80	10 $\bar{1}$ 2	6
3	4.81	24.34	1.690	1.685	0001(2)	1
2	5.21	26.38	1.560	1.544	00 $\bar{1}$ 3	6
				1.318	10 $\bar{1}$ 4	6
35	6.65	33.70	1.227	1.227	11 $\bar{2}$ 0	3
50	7.09	35.90	1.155	1.152	11 $\bar{2}$ 2	6
				1.138	10 $\bar{1}$ 5	6
				1.124	0001(3)	1
				1.062	10 $\bar{1}$ 0(2)	3
3	7.82	39.60	1.050	1.048	20 $\bar{2}$ 1	6
				1.008	10 $\bar{1}$ 1(2)	6
15	8.31	42.10	.990	{.994	10 $\bar{1}$ 6	6
				{.990	11 $\bar{2}$ 4	6
				.960	20 $\bar{2}$ 3	6
				.897	10 $\bar{1}$ 2(2)	6
				.877	10 $\bar{1}$ 7	6
				.842	0001(4)	1
				.833	20 $\bar{2}$ 5	6
2	10.06	51.0	.827	.829	11 $\bar{2}$ 6	6
5	10.41	52.8	.800	{.802	21 $\bar{3}$ 0	6
				{.797	21 $\bar{3}$ 1	12
				.783	10 $\bar{1}$ 8	6
				.780	21 $\bar{3}$ 2	12
				.773	10 $\bar{1}$ 3(2)	6
				.756	21 $\bar{3}$ 3	12
				.725	21 $\bar{3}$ 4	12
				.715	20 $\bar{2}$ 7	6
7	11.85	60.0	.712	{.708	10 $\bar{1}$ 0(3)	3
				{.708	10 $\bar{1}$ 9	6
15	12.11	31.4	.697	{.696	11 $\bar{2}$ 8	6
				{.693	30 $\bar{3}$ 2	6
				.690	21 $\bar{3}$ 5	12
1	12.61	64.0	.672	{.674	10 $\bar{1}$ 1(3)	6
				{.674	0001(5)	1
				.660	10 $\bar{1}$ 4(2)	6
9	12.94	65.6	.656	{.654	30 $\bar{3}$ 4	6
				{.654	21 $\bar{3}$ 6	12
				.644	10 $\bar{1}$ 10	6
1	13.79	69.8	.621	{.616	21 $\bar{3}$ 7	12
				{.616	11 $\bar{2}$ 0(2)	3
3	14.11	71.50	.609	{.612	2029	6
				{.612	2241	6

TABLE XIII.—Continued.

Intensity of Line.	Distance of Line from Center.	Angular Deviation of Line.	Spacing of Planes in Ångstroms.		Indices of Form	Number of Cooperating Planes.
			Experimental.	Theoretical.		
2	14.57	73.8	.592	.603	1121(2)	6
				.598	10 $\bar{1}\bar{2}$ (3)	6
				.592	2243	6
				.592	112 $\bar{1}$ 0	6

The crystallographic data regarding graphite is very meager and uncertain, and in attempting to guess its crystalline structure one has an embarrassing freedom of choice, both of crystal systems and of axial ratios and angles. The only guiding principles, apart from the lines in the photograph are, first, that the true structure is probably very simple and symmetrical, since all its atoms are alike, and second, that the nearest approach of adjacent atoms cannot be very different from that in diamond.

The structure whose spacings are tabulated in Table XIII. fits the experimental data best of all that have been tried, and seems capable, when account is taken of the internal structure of the atoms, of explaining all the observed intensities of the lines. It is a hexagonal structure, composed of four simple lattices of triangular prisms, each of side 2.47 Å. and height 6.80 Å., the atoms of the third lattice being directly above those of the first at a distance of one half the height of the prism, those of the 2d and 4th lattices being above the centers of alternate triangles of the first, at distances 1/14 and 8/14 respectively of the height of the prism. The coördinates of the atoms are:

$$\begin{array}{lll}
 m, & n, & pc, \\
 m + \frac{1}{3}, & n + \frac{2}{3}, & (p + \frac{1}{14})c, \\
 m, & n, & (p + \frac{1}{2})c, \\
 m + \frac{2}{3}, & n + \frac{1}{3}, & (p + \frac{8}{14})c,
 \end{array}$$

where m , n , and p have all possible values and c , the axial ratio, is 2.75. The 0001 planes are thus arranged in pairs, similar to the 111 planes in diamond. The distance between nearest consecutive planes, and between atoms in each plane, 4.8 Å. and 2.47 Å. respectively, are slightly less than their values .51 and 2.52 for diamond, and the nearest approach of atoms is 1.50 Å. as compared to 1.54 for diamond. This closer approach of the atoms in graphite would indicate chemical stability. The distance between consecutive pairs of planes, however, is much greater, viz., 3.40 Å. in graphite, than its value 2.06 Å. in diamond, which accounts for the extreme ease of basal cleavage and gliding in graphite.

The agreement between experimental and calculated spacings in Table XIII. is well within the limit of the experimental error, which is about 1 per cent. Every experimental spacing is accounted for, the first 12 with certainty, the last 7 with some ambiguity on account of the large number of theoretical spacings. The absence of reflection from planes such as $10\bar{1}4$, $10\bar{1}5$, the second orders of $10\bar{1}0$ and $10\bar{1}1$, and the third and fourth orders of 0001 , is dependent not only on the positions, but on the internal structure of the atoms, and cannot be interpreted except in conjunction with a study of this internal structure, which will be undertaken as soon as accurate photographic measurements can be obtained.

The structure given above has the lowest symmetry of any elementary substance yet studied. It may be that the essential elements of the hexagonal lattice can be more simply represented by a monoclinic or triclinic, or possibly an orthorhombic lattice, though efforts in this direction have so far been unsuccessful.

DIAMOND.

The crystal structure of diamond has been completely determined by the Braggs,¹ and confirmed by numerous observers. Comparison of the results of these investigators with those obtained from a powder photograph will therefore serve as an excellent check upon the latter. In addition, the powder photograph of diamond has a merit of its own, for it furnishes evidence not hitherto available regarding the internal structure of the most interesting of all atoms. The photographs taken thus far are not suitable for photometering, but arrangements are complete for taking such photographs, and for measuring the intensity of the lines.

Several photographs of diamond have been taken, under varying conditions, with identical results, as regards position and relative intensity of lines. Fig. 12 shows the result of a fifteen-hour exposure to Mo rays at 30,000 volts, 35 milliamperes, with zircon filter of 0.37 mm. A very thin wall glass tube of special lithium boro-silicate glass, 2 mm. in diameter, was filled with diamond powder, obtained by crushing some old dies in a steel mortar. This powder was mounted on the spectrometer table, concentric with a wooden disc 10.27 cm. in diameter, upon which Eastman X-ray film was fastened *in a complete circle*, except for a 5 mm. hole where the rays entered. The collimator slits were about 1.5 mm. wide, and the distance from X-ray target to powder was approximately 35 cm. Only one half of this film, corresponding to angles of diffraction from 0° to 180° , is shown in Fig. 12. Twenty-five of the possible 27 lines are visible in the photograph, the last two being obscured by the dense fog.

¹ X-Rays and Crystal Structure, p. 102 ff., Proc. Roy. Soc. A., 89, 277.

TABLE XIV.

Diamond.

Intensity of Line.	Distance of Line from Center x	Angular Deviation of Line θ .	Spacing of Planes in Angstroms.		Indices of Form.	Number of Cooperating Planes.
			Experimental.	Theoretical.		
1.00	1.80	20.06	2.05	2.06	111	4
.50	2.96	33.0	1.26	1.26	110	6
.40	3.49	39.92	1.072	1.075	311	12
.10	4.26	47.4	.885	.890	100	3
.25	4.66	52.0	.813	.817	331	12
.40	5.31	59.2	.721	.728	211	12
.20	5.66	63.0	.680	.683	{ 111(3) 511	16
.10	6.22	69.4	.625	.630	110(2)	6
.20	6.54	73.0	.597	.602	531	24
.15	7.10	79.2	.558	.563	310	12
.06	7.43	82.8	.538	.543	533	12
.03	7.98	89.0	.507	.513	111(4)	4
.08	8.24	91.8	.496	.498	{ 711 551	24
.20	8.76	97.6	.473	.476	321	24
.15	9.06	101.0	.462	.463	{ 731 553	36
.005	9.70	107.6	.442	.445	100(4)	3
.003	10.00	113.2	.432	.435	733	12
.12	10.52	116.8	.417	.420	{ 411 110(3)	18
.08	10.84	120.8	.409	.411	{ 751 111(5)	28
.05	11.50	127.6	.397	.397	210	12
{ .08 .02	{ 11.84 11.93	{ 132.0 132.8	.389	.391	{ 753 911	36
{ .05 .01	{ 12.54 12.70	{ 139.8 141.4				
{ .05 .01	{ 13.00 13.23	{ 145.0 147.2	.378	.379	332	12
{ .07 .02	{ 14.00 14.27	{ 156.0 159.0				
{ .20 .06	{ 14.83 15.35	{ 165.4 171.2	.372	.373	931	24
			.363	.363	211(2)	12
			.358	.358	{ 933 755 771 311(3)	48

The lines and the corresponding spacings are tabulated in Table XIV., and compared with those required for the lattice which has been assigned to diamond by the Braggs. The agreement is absolute. It will be noted that for the larger deviations the doublet of the molybdenum radiation is clearly resolved.

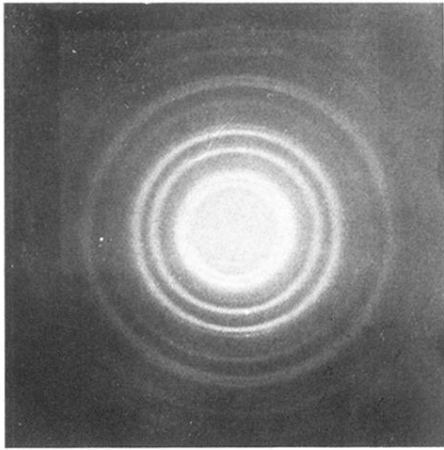


FIG. 1. Aluminium.

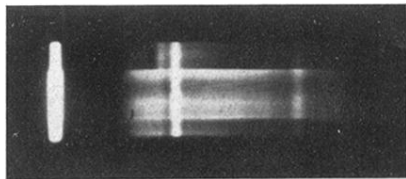


FIG. 5. Tungsten X-Ray Spectrum.

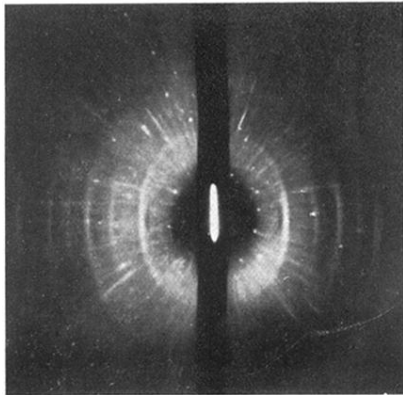


FIG. 6. Iron.

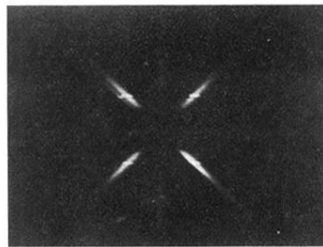


FIG. 7a. Silicon Steel.

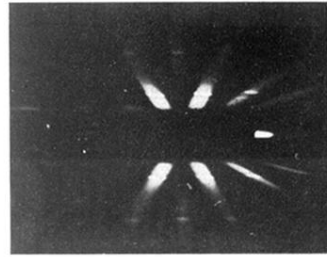


FIG. 7b. Silicon Steel.

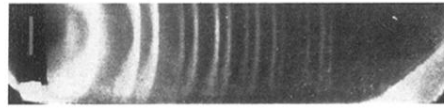


FIG. 8. Silicon.

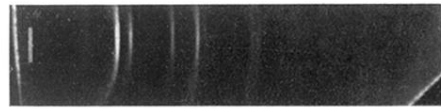


FIG. 9. Aluminum.

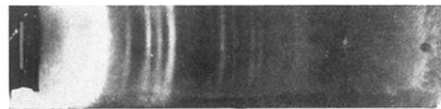


FIG. 10. Magnesium.

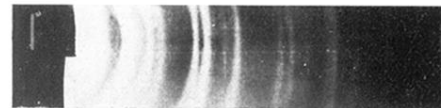


FIG. 11. Graphite.

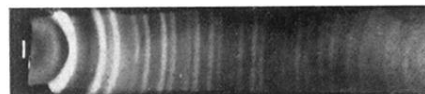


FIG. 12. Diamond.